

Germline MBD4 Mutations and Predisposition to Uveal Melanoma

Anne-Céline Derrien, Manuel Rodrigues, Alexandre Eeckhoutte, Stéphane Dayot, Alexandre Houy, Lenha Mobuchon, Sophie Gardrat, Delphine Lequin, Stelly Ballet, Gaëlle Pierron, et al.

▶ **To cite this version:**

Anne-Céline Derrien, Manuel Rodrigues, Alexandre Eeckhoutte, Stéphane Dayot, Alexandre Houy, et al.. Germline MBD4 Mutations and Predisposition to Uveal Melanoma. JNCI: Journal of the National Cancer Institute, 2020, pp.djaa047. 10.1093/jnci/djaa047 . inserm-03034626

HAL Id: inserm-03034626

https://inserm.hal.science/inserm-03034626

Submitted on 1 Dec 2020

HAL is a multi-disciplinary open access archive for the deposit and dissemination of scientific research documents, whether they are published or not. The documents may come from teaching and research institutions in France or abroad, or from public or private research centers.

L'archive ouverte pluridisciplinaire **HAL**, est destinée au dépôt et à la diffusion de documents scientifiques de niveau recherche, publiés ou non, émanant des établissements d'enseignement et de recherche français ou étrangers, des laboratoires publics ou privés.

OXFORD

JNCI J Natl Cancer Inst (2020) 113(1): djaa047

doi: 10.1093/jnci/djaa047
First published online April 1, 2020
Article

Germline *MBD4* Mutations and Predisposition to Uveal Melanoma

Anne-Céline Derrien, MSc,[1,‡] Manuel Rodrigues, MD, PhD,[1,2,‡] Alexandre Eeckhoutte, BSc,[1] Stéphane Dayot, BSc,[1] Alexandre Houy, BSc,[1] Lenha Mobuchon, PhD,[1] Sophie Gardrat, MD,[1,3] Delphine Lequin, MD,[3] Stelly Ballet, MSc,[3] Gaëlle Pierron, PhD,[3] Samar Alsafadi, PharmD,[1,4] Odette Mariani, PhD,[5] Ahmed El-Marjou, PhD,[6] Alexandre Matet, MD, PhD,[7,8] Chrystelle Colas, MD, PhD,[9] Nathalie Cassoux, MD, PhD,[7,8] Marc-Henri Stern, MD, PhD[1,9,*]

[1]Inserm U830, DNA Repair and Uveal Melanoma (D.R.U.M.), Equipe Labellisée Par la Ligue Nationale Contre le Cancer, Paris, France; [2]Department of Medical Oncology, Institut Curie, PSL Research University, Paris, France; [3]Department of Biopathology, Institut Curie, PSL Research University, Paris, France; [4]Translational Research Department, Institut Curie, PSL Research University, Paris, France; [5]Biological Resource Center, Institut Curie, PSL Research University, Paris, France; [6]Institut Curie, PSL Research University, UMR144, Recombinant Protein Facility, Paris, France; [7]Department of Ocular Oncology, Institut Curie, Paris, France; [8]Faculty of Medicine, University of Paris Descartes, Paris, France and [9]Department of Genetics, Institut Curie, Paris, France

[*]**Correspondence to:** Marc-Henri Stern, MD, PhD, 26 rue d'Ulm, 75248 Paris cedex 05, France (e-mail: marc-henri.stern@curie.fr).
[‡]Authors contributed equally to this work.

Abstract

Background: Uveal melanoma (UM) arises from malignant transformation of melanocytes in the uveal tract of the eye. This rare tumor has a poor outcome with frequent chemo-resistant liver metastases. *BAP1* is the only known predisposing gene for UM. UMs are generally characterized by low tumor mutation burden, but some UMs display a high level of CpG>TpG mutations associated with *MBD4* inactivation. Here, we explored the incidence of germline *MBD4* variants in a consecutive series of 1093 primary UM case patients and a series of 192 UM tumors with monosomy 3 (M3). **Methods:** We performed *MBD4* targeted sequencing on pooled germline (n = 1093) and tumor (n = 192) DNA samples of UM patients. *MBD4* variants (n = 28) were validated by Sanger sequencing. We performed whole-exome sequencing on available tumor samples harboring *MBD4* variants (n = 9). Variants of unknown pathogenicity were further functionally assessed. **Results:** We identified 8 deleterious *MBD4* mutations in the consecutive UM series, a 9.15-fold (95% confidence interval = 4.24-fold to 19.73-fold) increased incidence compared with the general population (Fisher exact test, $P = 2.00 \times 10^{-5}$, 2-sided), and 4 additional deleterious *MBD4* mutations in the M3 cohort, including 3 germline and 1 somatic mutations. Tumors carrying deleterious *MBD4* mutations were all associated with high tumor mutation burden and a CpG>TpG hypermutator phenotype. **Conclusions:** We demonstrate that *MBD4* is a new predisposing gene for UM associated with hypermutated M3 tumors. The tumor spectrum of this predisposing condition will likely expand with the addition of *MBD4* to diagnostic panels. Tumors arising in such a context should be recognized because they may respond to immunotherapy.

Uveal melanoma (UM) is the most frequent primary intraocular tumor in adults with an overall mean incidence of 5.2 per million per year in the United States (1). Metastases arise in more than 30% of case patients, almost invariably in the liver, with a dismal prognosis because of the absence of effective treatment (median survival of 10 months) (2,3). UMs with high risk of developing metastases are characterized by loss of chromosome 3 and by *BAP1* (encoded in 3p21) inactivation resulting from loss-of-function (LoF) mutations and loss of the remaining wild-type copy on chromosome 3 (4). Rare familial UMs are associated with germline mutations of *BAP1* (Mendelian Inheritance in Man [MIM]: 614327) (5,6), which is the only known highly penetrant UM predisposition gene. UM mainly affects individuals of European ancestry and is associated with fair skin and light iris color. However, the low tumor mutation burden (TMB) and lack of an ultraviolet-associated mutational signature argue against a role for ultraviolet radiation in UM oncogenesis (7).

Recently, the characterization of a metastatic UM patient with an exceptional response to anti-Programmed cell death protein 1 (anti-PD-1) therapy led us to identify a CpG>TpG mutator phenotype linked to germline protein truncating variants (PTV) in *MBD4* (Methyl-CpG Binding Domain Protein 4) and somatic loss of the wild-type allele in tumors in 2 patients with UM and 1 with glioma (8). Another UM patient responding to

Received: December 20, 2019; **Revised:** March 19, 2020; **Accepted:** March 26, 2020

© The Author(s) 2020. Published by Oxford University Press.
This is an Open Access article distributed under the terms of the Creative Commons Attribution-NonCommercial-NoDerivs licence (http://creativecommons.org/licenses/by-nc-nd/4.0/), which permits non-commercial reproduction and distribution of the work, in any medium, provided the original work is not altered or transformed in any way, and that the work is properly cited. For commercial re-use, please contact journals.permissions@oup.com

Downloaded from https://academic.oup.com/jnci/advance-article/doi/10.1093/jnci/djaa047/5810647 by guest on 01 December 2020

ARTICLE

immune checkpoint inhibitors was subsequently reported with a germline *MBD4* PTV (9). *MBD4* encodes a glycosylase involved in the base excision repair of DNA damage arising from spontaneous deamination of 5-methylcytosine to thymine (10,11), which is consistent with the mCpG>TpG transitions [mutational signature SBS1 (12)] observed in *MBD4*-inactivated tumors (12). *MBD4*, located on chromosome 3, is thought to act as a tumor suppressor gene, following Knudson's 2-hit model with loss of the wild-type allele by monosomy 3 (M3) in UMs (8). Altogether, these germline deleterious *MBD4* variants in UM prompted us to investigate the role of *MBD4* as a predisposing gene for UM. Here, we performed *MBD4* targeted-sequencing in germline DNA of a large consecutive series of 1093 UM patients and in tumor DNA of a second cohort of 192 UM patients with M3 and investigated the TMB and mutational signature in patients harboring *MBD4* mutations.

Methods

Study Patients

The 1099 individuals with UM were diagnosed at Institut Curie, France, from 2013 to 2018. The sex proportion of female to male was 52.2 to 47.8 ± 3.0% (95% confidence interval [CI]) and the median age at diagnosis was 64 years old (Q1-Q3 quartile interval = 54-73). All patients provided written informed consent to perform germline genetic analyses and somatic genetic analyses of tumor samples. Six patients were subsequently removed from the study: the UM diagnosis was not confirmed for 5 patients, and the sixth patient had undergone a bone marrow transplantation and his blood sample corresponded to his donor's (Supplementary Figure 1A, available online). The study was conducted in accordance with the declaration of Helsinki and was approved by the ethical committee and institutional review board of the Institut Curie. Germline DNA was extracted from the blood of all patients (DNeasy Blood and Tissue kit, Qiagen). When available, tumor genomic status as part of the prognostication assessment was extracted from the medical record and classified as M3, including isodisomy 3) or disomy 3 (D3). Tumor samples were collected from primary eye tumors. A second series of 192 UM tumor samples with M3 was also accrued at Institut Curie, of which 120 patients were independent from the consecutive germline cohort.

MBD4 Targeted Sequencing

Germline DNA of 1099 UM patients from the UM consecutive series (before removal of the 6 a forementioned patients) and DNA of a series of 192 M3 UM tumors were screened for *MBD4* variants by pooled *MBD4* targeted sequencing. Details on the sequencing strategy and bioinformatics pipeline are described in the Supplementary Methods (available online). Deconvolution of the identified pooled DNA samples with an *MBD4* variant was carried out by Sanger sequencing.

Identified *MBD4* variants (Supplementary Table 1, available online) were defined following the recommendations of the Human Genome Variation Society (http://varnomen.hgvs.org/) and numbered based on the *MBD4* (MIM: 603574) cDNA and protein sequences (GenBank accession numbers NM_003925.2 and NP_003916.1, respectively).

Glycosylase Activity Assay

Wild-type and mutant MBD4 were expressed to assess their enzymatic activity by in vitro MBD4 glycosylase assay as previously described (13,14) (Supplementary Methods, available online).

Whole-Exome Sequencing (WES) and Mutation Calling

WES was performed on tumor samples from *MBD4* variant carriers who consented to germline studies (Supplementary Table 2, available online). Variant calling and TMB analysis are described in Supplementary Methods (available online).

Statistical Analysis

Statistical analysis was performed using R software v3.6. Fisher exact test was used to calculate *P* values between our cohort and the general population. Random subsampling 1 000 000 times of 2186 alleles from the GnomAD cohort was also used as statistical "matching" strategy to calculate *P* values between our cohort and the general population. A Mann-Whitney *U* test was used to compare the median ± median absolute deviation for the mutation burden and CpG>TpG proportion between MBD4-deficient ($MBD4_{def}$) and MBD4-proficient patients. To compare age of UM onset, a Wilcoxon Rank-Sum test was used. For survival analysis using Kaplan-Meier curves, statistical analysis was carried out using the log-rank test. All statistical tests were 2-sided, except for 1-sided Wilcoxon Rank-Sum test for early age of onset in $MBD4_{def}$ patients. Confidence intervals were carried out at 95% confidence level. Confidence intervals for relative risk (RR) measurement was calculated as previously described (15). A *P* value less than .05 was considered to be statistically significant.

Results

Mining *MBD4* Germline Variants in Public UM Cohorts

To evaluate the potential predisposing role of *MBD4* in UM, we mined all available public UM cohorts for germline *MBD4* variants. We identified 1 case harboring the germline deleterious *MBD4* PTV c.1443delT (p.Leu482Trpfs*9) in a first cohort containing 37 UM patients (phs001421.v1.p1) (16). A second cohort of 98 UM patients (phs000823.v1.p1) included a second case with an *MBD4* c.1020delA (p.Asp341Thrfs*13) PTV. Collectively, 5 *MBD4* germline deleterious variants were found in 268 analyzed UM patients (1.9%) (8,9,16–18). In contrast, such variants are exceedingly rare in an unselected population (88 of approximately 125 000 individuals in GnomAD v2.1.1). Out of these 5 UM case patients with germline *MBD4* variants, 4 had available tumor profiles that all showed M3 and somatic *BAP1* inactivation (8,9,16), presumably because of the localization of both *MBD4* and *BAP1* on chromosome 3.

Identification of *MBD4* Germline Variants in the In-House Consecutive UM Series

To assess the actual prevalence of *MBD4* germline deleterious variants in UM, we next explored an in-house cohort of 1093 (approximately one-half the annual incidence in United States) consecutive patients diagnosed with UM at Institut Curie between 2013 and 2018. Targeted next-generation sequencing in

ARTICLE

Downloaded from https://academic.oup.com/jnci/advance-article/doi/10.1093/jnci/djaa047/5814932 by guest on 01 December 2020

pooled patient DNA followed by Sanger sequencing revealed germline *MBD4* PTVs in 7 patients (Table 1): 2 splice site variants (c.1562-1G>T [p.Asp521Profs*4] in 2 patients and a c.335 + 1G>A [p.Arg83Profs*5] variant), 2 frameshift deletion variants (c.1443delT [p.Leu482Trpfs*9] and c.1384delG [p.Ala462Leufs*29]), and 1 stop-gain near the end of the last exon of *MBD4* (c.1706G>A [p.Trp569*] in 2 patients).

We also identified and characterized 9 rare germline *MBD4* variants (frequency <1% in the general population): 7 missense variants in 13 patients and 2 intronic variants in 2 patients (Figure 1A). Out of these, 3 were predicted with possible splicing consequences: 2 missense variants (c.1652A>G [p.Asn551Ser] and c.1400A>G [p.Asn467Ser]), and 1 intronic variant (c.1277-18T>A) (Supplementary Table 1, available online).

Functional Assessment of *MBD4* Variants

Exon-trapping assays performed on the 3 aforementioned variants demonstrated the use of an alternative acceptor site with c.1277-18T>A, albeit to a lesser extent than the canonical splice site, whereas c.1652A>G and c.1400A>G did not show any measurable effect (Supplementary Figure 2, available online).

All missense variants within the MBD4 glycosylase domain [aa425-580] were assessed by in vitro glycosylase assay together with p. Trp569* because of its localization near the end of the protein (Figure 1; Table 1). The assay confirmed that p. Trp569* results in a catalytically inactive protein and further demonstrated p. Arg468Trp to be a LoF variant (Figure 1). Consistent with this finding, the key role of Arg468 was previously established in binding at the G/T mismatch site, maintaining the T base in a position required for catalysis, and interacting with the orphan G base through hydrogen bonding (22).

We next characterized by WES the 3 available tumors from patients carrying germline *MBD4* LoF variants (UM75: p. Trp569*, UM605: p. Ala462Leufs*29, and UM656: p. Leu482Trpfs*9) (8). We confirmed that the 3 *MBD4* germline LoF mutations were associated with somatic loss of the wild-type allele in the tumors by either M3 (UM75 and UM605) or isodisomy 3 (UM656) (Figure 1C; Supplementary Table 1, available online), consistent with the 3q21.3 location of *MBD4*.

MBD4 Mutations in the M3 Tumor Series and Tumor Signature

To further evaluate the incidence of *MBD4* alterations in UM, and assuming that $MBD4_{def}$ UMs are associated with M3, we accrued a series of 192 UM tumor samples with M3 (of which 120 case patients were independent from the present consecutive UM series) and screened for *MBD4* mutations using the aforementioned strategy (Supplementary Figure 1B, available online). We identified 6 additional *MBD4* variants, including 4 LoF mutations (UMT62: c.1688T>A [p.Leu563*], UMT45: c.1562-1G>T [p.Asp521Profs*4], UMT61: c.1002delTTTG [p.Lys335Phefs*18], UMT162: c.541C>T [p.Arg181*]) and 2 missense variants (UMT88: c.1402C>T [p.Arg468Trp] and UMT105: c.1073T>C [p.Ile358Thr]) (Table 1; Figure 1; Supplementary Table 1, available online). Of these, 4 patients (UMT45, UMT61, UMT162, and UMT88) had available germline DNA and all consented to germline studies. Characterization by WES of their tumor samples showed that the 3 tested LoF mutations were germline variants, the missense p. Arg468Trp was somatic, and all were associated with Loss Of Heterozygosity (LOH) of the wild-type allele in tumors (Figure 1, A and B; Supplementary Table 1, available online).

MBD4 inactivation has been associated with a high TMB and a CpG>TpG mutational pattern (8). We confirmed the high TMB in all 3 available $MBD4_{def}$ UMs from the germline consecutive cohort with 275, 122, and 181 variants per exome in UM75, UM605, and UM656, respectively, compared with 16 ± 4.0 (median ± median absolute deviation) variants in MBD4-proficient UMs (18) (Figure 1C; Supplementary Table 2, available online). CpG>TpG transitions represented 96.4%, 85.7%, and 92.8% of all single nucleotide variants (SNVs), respectively, compared with 24.3 ± 7.6% in MBD4-proficient UMs (18) (Figure 1, C and D; Supplementary Table 2, available online). In line with the glycosylase assay, TMB results and somatic chromosome 3 LOH further confirmed the deleterious effect of p. Trp569* in UM75 (Figure 1). Similarly, within the M3 UM tumor series, the 3 available UMs carrying a germline LoF *MBD4* variant exhibited a high TMB (269, 288, and 86 variants per exome in UMT162, UMT45, and UMT61, respectively) and a predominance of CpG>TpG transitions (85.6%, 94.4%, and 63.9%, respectively) among all SNVs (Figure 1, C and D; Supplementary Table 2, available online). The tumor sample of patient UMT88, carrying a somatic p. Arg468Trp variant identical to that found as a germline variant in UM293, also carried a high TMB (243 variants) and the CpG>TpG mutational pattern (92.5%) (Figure 1, C and D; Supplementary Table 2, available online), thereby confirming the deleterious effect of this missense variant previously demonstrated in the glycosylase assay (Figure 1). Taken together, these 7 patients with *MBD4* deleterious mutations had a 15-fold increase in number of variants per exome ($MBD4_{def}$: 243 ± 66.7 variants vs $MBD4_{pro}$: 16 ± 4.0, Mann-Whitney $P = 8.72 \times 10^{-5}$) and a statistically significantly higher CpG>TpG median proportion among SNVs ($MBD4_{def}$: 92.5 ± 5.7% vs $MBD4_{pro}$: 24.3 ± 7.5%, $P = 9.82 \times 10^{-7}$) (18).

In addition, we characterized the available tumor samples from 2 patients harboring missense variants that were not predicted to be deleterious (UM102: c.139G>A [p.Gly47Arg] and UM350: c.1652A>G [p.Asn551Ser]; Figure 1; Supplementary Table 1; Supplementary Figure 2, available online). The low TMB (33 and 40 variants per exome, respectively) and absence of CpG>TpG signature confirmed their neutral effect (Supplementary Table 2; Supplementary Figure 3, available online).

Incidence of Germline *MBD4* Deleterious Mutations in UM

Taken together, we thus identified 8 LoF germline variants in *MBD4* among the 1093 consecutive UM case patients, including p. Arg468Trp with deleterious effect on MBD4 glycosylase activity (Table 1). These account for a statistically significant 9.15-fold increase in deleterious variant frequency compared with the general population, even when restricting ourselves to truncating and splicing *MBD4* LoFs as defined by GnomAD (7 LoFs of 2186 observed alleles in UM, representing a variant allele frequency [VAF] of 0.0032 vs 88 LoFs out of a median of 251 450 alleles in the GnomAD v2.1 general population; VAF = 3.50×10^{-4}; Fisher exact test $P = 2.00 \times 10^{-5}$). To circumvent the imbalanced dataset, a "matching" subsampling approach was used, giving a similar *P* value (1.60×10^{-5}). Therefore, we demonstrate that the prevalence of *MBD4* germline deleterious variants in UM is approximately 0.7%, close to that of *BAP1* germline mutation in UM (1.6%) (23), and that *MBD4* mutations strongly predispose to UM with an RR of 9.15 (95% CI = 4.24 to 19.73). A comparison between *MBD4* germline LoF frequency in

Downloaded from https://academic.oup.com/jnci/advance-article/doi/10.1093/jnci/djaa047/5810697 by guest on 01 December 2020

ARTICLE

Table 1. *MBD4* germline deleterious variants in UM and in other malignancies[a]

Patient series	Patient	Variant	dbSNP	Mutation type	Glycosylase assay	GnomAD allele frequency (NFE[b])		
						Allele count	Obs. allele number	Frequency
UM[e] germline consecutive series	UM75	p.Trp569*	rs939751619[c]	stop_gain	Inactive[d]	2	129 130	1.55×10^{-5}
	UM1033							
	UM49	p.Asp521Profs*4	rs778697654[c]	splice_acceptor	ND	5	113 766	4.39×10^{-5}
	UM1088							
	UM656	p.Leu482Trpfs*9	rs769076971[c]	frameshift_deletion	ND	3	113 752	2.64×10^{-5}
	UM293	p.Arg468Trp	rs1380952147	nonsynonymous_SNV	Inactive[d]	0	113 630	0.00
	UM605	p.Ala462Leufs*29	–	frameshift_deletion	ND	—	—	—
	UM436	p.Arg83Profs*5	rs552296498[c]	splice_donor	ND	3	129 158	2.32×10^{-5}
UM M3 tumor series	UMT45	p.Asp521Profs*4	rs778697654[c]	splice_acceptor	ND	5	113 766	4.39×10^{-5}
	UMT61	p.Lys335Phefs*18	rs1443006605	frameshift_deletion	ND	0	113 650	0,00
	UMT162	p.Arg181*	rs1270271346	stop_gain	ND	2	128 972	1.55×10^{-5}
UM (public data)	UM (9)	p.Leu563*	rs200758755	stop_gain	ND	8	113 702	7.04×10^{-5}
	TCGA_UVM_1 (8)	p.Asp521Profs*4	rs778697654[c]	splice_acceptor	ND	5	113 766	4.39×10^{-5}
	$UM_{phs001421.v1.p1}$ (16)	p.Leu482Trpfs*9	rs769076971[c]	frameshift_deletion	ND	5	113 752	4.40×10^{-5}
	UVM_IC (8)							
	$UM_{phs000823.v1.p1}$	p.Asp341Thrfs*13	–	frameshift_deletion	ND	—	—	—
Other malignancies	$AML_{EMC\text{-}AML\text{-}1}$ (13)	p.His567del	rs775848563	inframe_deletion	ND	—	—	—
	$AML_{WEHI\text{-}AML\text{-}1/2}$ (13)	p.Asp521Profs*4	rs778697654[c]	splice_acceptor	ND	5	113 766	4.39×10^{-5}
	$AML_{WEHI\text{-}AML\text{-}1/2}$ (13)	p.Glu314Argfs*13	rs558765093[c]	frameshift_insertion	ND	—	—	—
	Spiradenocarcinoma (19)							
	TCGA_GBM_4 (8)	p.Arg83Profs*5	rs552296498[c]	splice_donor	ND	3	129 158	2.32×10^{-5}
	Colorectal polyposis (20)	p.Gln73*	rs148098584	stop_gain	ND	0	113 750	0.00
	Pilocytic astrocytoma (21)	NA[g]	NA	NA	ND	NA	NA	NA
	Gastric adenocarcinoma (21)	NA	NA	NA	ND	NA	NA	NA
	Pancreatic adenoK (21)	NA	NA	NA	ND	NA	NA	NA
	Pancreatic endocrine tumor (21)	NA	NA	NA	ND	NA	NA	NA

[a]adenoK = adenocarcinoma; AML = acute myeloid leukemia; GBM = glioblastoma; M3 = monosomy 3; NA = not available; ND = not determined; NFE = non-Finnish European; UM or UVM = uveal melanoma; — = no value given because of the absence of the variant in dbSNP and/or in the GnomAD NFE population.
[b]NFE population of the Genome Aggregation Database (GnomAD v2.1.1).
[c]Variant found in more than 1 nonrelated patient.
[d]Inactive: absence of glycosylase activity of the recombinant protein carrying the variant.

Downloaded from https://academic.oup.com/jnci/advance-article/doi/10.1093/jnci/djaa047/5814932 by guest on 01 December 2020

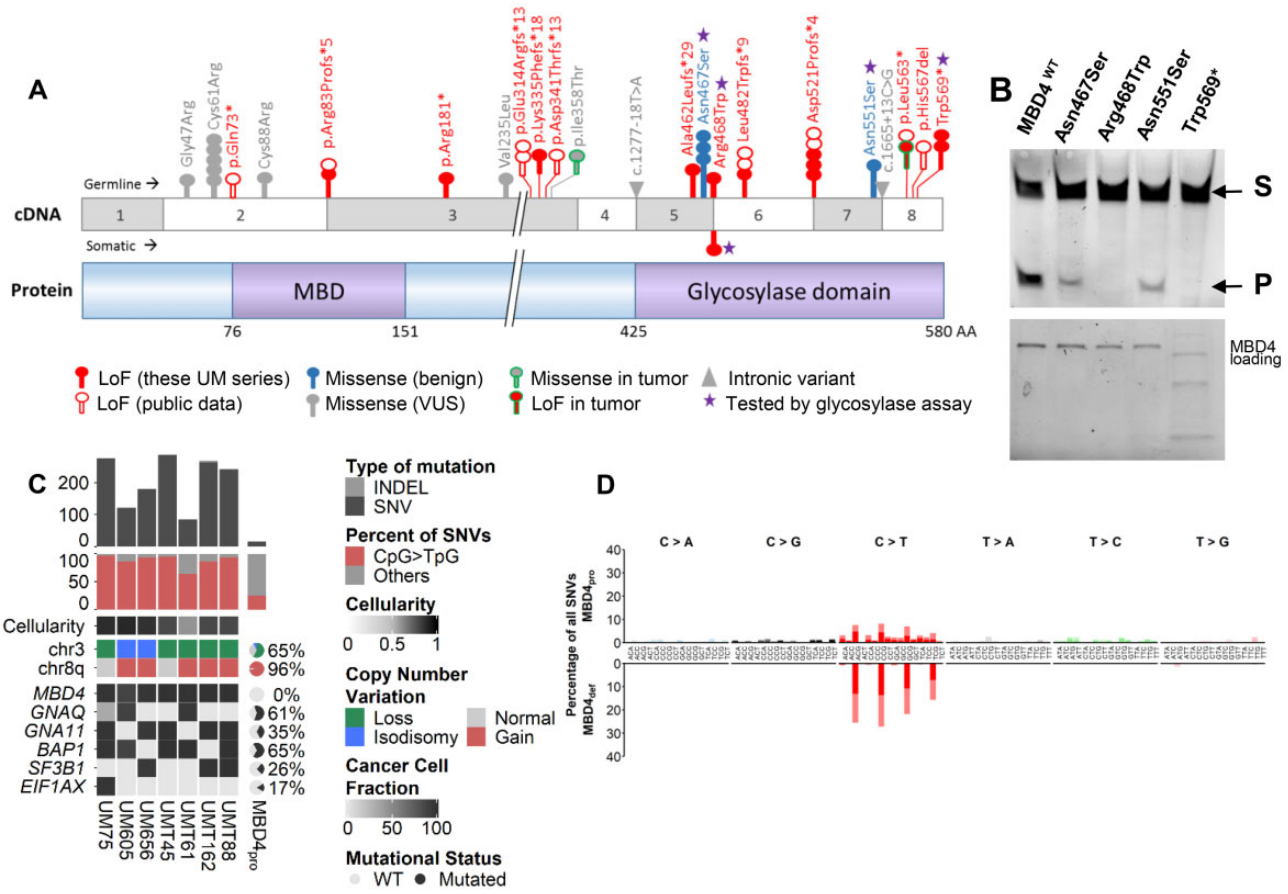


Figure 1. Functional consequences and phenotype associated with germline and somatic *MBD4* deleterious variants. **A)** Schematic representation of *MBD4* cDNA (**top**) and protein (**bottom**) sequences. Functional methyl-binding domain (MBD) and glycosylase domain are indicated. The position of all *MBD4* variants identified in the 2 uveal melanoma (UM) series (consecutive germline UM series and tumor monosomy 3 [M3] series) is highlighted, with germline and somatic variants above and below the cDNA sequence, respectively, and the 2 variants from the tumor M3 cohort with unknown somatic or germline origin circled in **green**. These *MBD4* variants include loss-of-function (LoF, in **red**), missense (either benign, in **blue-filled circles**, or of unknown biological significance [VUS] in **gray-filled circles**) and intronic (**gray triangles**) variants. Each circle represents 1 patient harboring the variant. Other *MBD4* germline deleterious variants mined on public data are also shown (**empty red circles**). **B) Top**: Glycosylase activity assay of recombinant wild-type MBD4 ($MBD4^{WT}$) and mutant proteins resulting from missense variants and 1 stop gain variant (**purple star** in 1A) residing in the MBD4 glycosylase domain. Substrate = S; cleaved product = P. **Bottom**: loading blot for MBD4 wild-type and mutant recombinant proteins corresponding to the glycosylase assay. **C)** Tumor characteristics of *MBD4*-deficient ($MBD4_{def}$) patients compared with that of *MBD4*-proficient UM patients ($MBD4_{pro}$) (18). $MBD4_{def}$ patients include UM75, UM605, and UM656 from the consecutive germline series and UMT45, UMT61, UMT162, and UMT88 from the M3 UM tumor series. All patients harbor germline *MBD4* variants, except for UMT88 with a somatic *MBD4* variant. **Top**: tumor mutation burden estimated by number of variants (single nucleotide variants [SNVs] in **dark gray**, and insertions-deletions [INDELs] in **light gray**) in the exome; **middle**: proportion of CpG>TpG transitions (**red**) relative to all SNVs (**gray**); **bottom**: copy number alterations in chromosomes 3 and 8q, and mutational status *of MBD4*, *GNAQ*, *GNA11*, *BAP1*, *SF3B1*, and *EIF1AX*, represented as percentage for the $MBD4_{pro}$ series (18). The clonality or subclonality of these key mutational events is indicated by their cancer cell fraction in **black-gray gradation**, taking into account the variant allele frequency (VAF), copy number change, and cellularity. A plot of the VAF distribution of all variants in the 7 exomes is available in Supplementary Figure 4 (available online). For each exome in the $MBD4_{def}$ group, tumor cellularity is indicated by **black-gray shading** (and quantified in Supplementary Table 2, available online). **D)** Mutational patterns of the $MBD4_{def}$ (**top**) and $MBD4_{pro}$ (**bottom**) groups based on the relative proportion (**y-axis**) of each of the 96 types of trinucleotide substitution (**x-axis**). **Dark or bright colors** correspond to sense or antisense strands. Individual mutational pattern for all tumor exomes assessed are available in Supplementary Figure 3 (available online).

this UM consecutive series and in different subsets of the GnomAD population (in the general and European populations) is further presented in Table 2.

Within the UM tumor cohort with M3, we identified a total of 5 *MBD4* LoF variants, including at least 3 of germline origin and 1 somatic, out of 192 UM patients. These 3 germline LoF variants by themselves account for a VAF of 0.016, more than twice that found in the germline consecutive UM cohort. This was expected given the recurrence of approximately 50% of chromosome 3 loss event among all UM patients (24). This finding confirms that *MBD4* deficiency in UM is mainly associated with M3 and that *MBD4* germline mutations specifically predispose to hypermutated high-risk M3 UMs.

Defining the *MBD4* Predisposition Syndrome

To further characterize this new cancer predisposition, we investigated the medical records of *MBD4* mutation carriers. In contrast with the high RR of 9.15 (and therefore an approximately 9-fold higher risk of developing a UM) conferred by *MBD4* LoF germline mutations, none of these individuals had familial or bilateral UM. With a lifetime risk of UM estimated at 7.69×10^{-5} in the general population (25), an RR of 9 would result in a lifetime risk of UM of 6.92×10^{-4}. Such incidence is still too low to observe familial aggregation, which is consistent with our finding. Assuming that all $MBD4_{def}$ UMs are associated with M3, we compared their medical records with patients from this cohort with available tumor

Downloaded from https://academic.oup.com/jnci/advance-article/doi/10.1093/jnci/djaa047/5813647 by guest on 01 December 2020

Table 2. Frequency of *MBD4* germline deleterious variants in the UM series compared with various populations of the GnomAD database[a]

Study population		No. of LoF variants	Allele count[c]	Frequency	RR[d](95% CI[e])	Fisher test (*P* value)
UM consecutive series		7[f]	2186	0.00320	—	—
GnomAD v2.1.1	NFE[b]	47	113 736	0.00041	7.75 (3.51 to 17.12)	6.86×10^{-5}
	Population[b]	88	251 450	0.00035	9.15 (4.24 to 19.73)	2.00×10^{-5}
GnomAD v2.1.1 (controls only)	NFE	13	42 768	0.00030	10.53 (4.20 to 26.38)	2.82×10^{-5}
	General population	33	109 404	0.00030	10.62 (4.70 to 23.97)	1.16×10^{-5}
GnomAD v2.1.1 (noncancer only)	NFE	41	102 730	0.00040	8.02 (3.60 to 17.86)	5.89×10^{-5}
	General population	82	236 912	0.00035	9.25 (4.28 to 19.99)	1.90×10^{-5}
GnomAD v3	NFE	20	64 571	0.00031	10.34 (4.38 to 24.42)	2.00×10^{-5}
	General population	39	143 286	0.00027	11.76 (5.27 to 26.27)	5.50×10^{-5}

[a]CI = confidence interval; LoF = loss-of-function (deleterious) variants; NFE = non-Finnish European; RR = relative risk; UM = uveal melanoma; — = no value given here because the relative risk, confidence interval, and statistic tests are presented between the UM consecutive series and each GnomAD subpopulation in the rows below.
[b]NFE population subset of the Genome Aggregation Database (GnomAD v2.1.1).
[c]For all GnomAD populations described, refers to the median number of allele count.
[d]RR here is calculated by dividing the LoF frequency in the UM consecutive series by the LoF frequency in the corresponding GnomAD population subset.
[e]Confidence interval of the relative risk is calculated as previously described (15).
[f]Seven LoF variants correspond to the 8 deleterious *MBD4* variants identified in this study, with removal of the missense deleterious variant p. Arg468Trp so as to restrict the analysis to LoF variants as defined by GnomAD for accurate comparison.

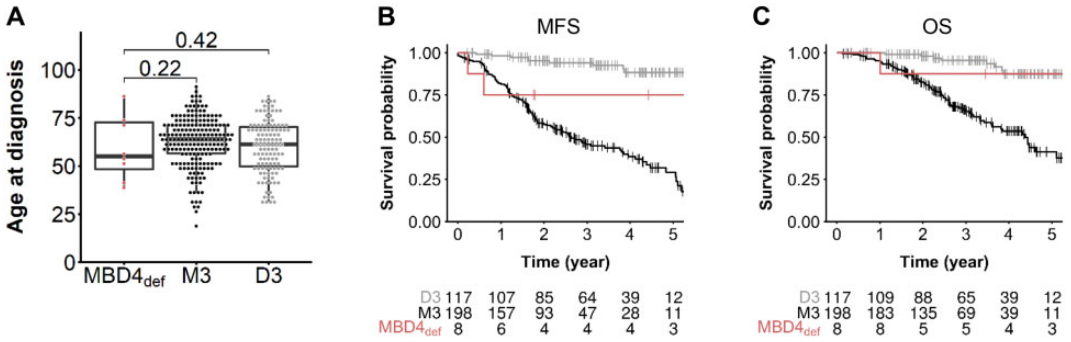


Figure 2. Uveal melanoma (UM) clinical characteristics in an MBD4-deficient ($MBD4_{def}$) context. **A)** Age of UM onset of $MBD4_{def}$ patients (n = 8) in the germline consecutive UM series compared with disomy 3 (D3, n = 117) and monosomy 3 (M3, n = 198) MBD4-proficient ($MBD4_{pro}$) UMs. Wilcoxon test, 1-sided (testing early UM onset in $MBD4_{def}$ patients): $MBD4_{def}$ vs M3: P = .22, $MBD4_{def}$ vs D3: P = .42; no age difference found between D3 and M3 groups, Wilcoxon test, 2-sided P = .087; – not shown). **B and C)** Metastasis-free survival (MFS, B) and overall survival (OS, C) of $MBD4_{def}$ UM patients (n = 8) and $MBD4_{pro}$ UM patients with M3 or D3. Time zero refers to time at primary UM diagnosis. MFS was defined as the interval between the date of primary UM diagnosis and the date of distant metastasis (first imaging) or death from any cause. The number of patients in each group at each time point (year) is indicated. Survival distributions were estimated by the Kaplan-Meier method and compared using the log-rank test: log-rank test, 2-sided, M3 vs D3: $P = 1.98 \times 10^{-9}$ (OS), $P = 1.11 \times 10^{-16}$ (MFS); M3 vs $MBD4_{def}$: P = .11 (OS), P = .06 (MFS); D3 vs $MBD4_{def}$: P = .62 (OS), P = .10 (MFS).

genomic status, that is, 198 *MBD4* wild-type M3 and 117 *MBD* wild-type D3 UMs. Surprisingly, no early-onset UM was found in *MBD4* carriers compared with noncarriers regardless of their chromosome 3 status ($MBD4_{def}$: median age and Q1-Q3 quartile interval = 55.5, 95% CI = 48.4 to 72.8, N = 8; D3: 61.3, 95% CI = 49.8 to 70.3, N = 117; M3: 63.4, 95% CI = 56.6 to 71.4, N = 198; Wilcoxon test, 1-sided: $MBD4_{def}$ vs M3: P = .22, $MBD4_{def}$ vs D3: P = .42; no age difference found between D3 and M3 groups, Wilcoxon test, 2-sided P = .087; Figure 2A). Although the size of the $MBD4_{def}$ series prevents any definitive conclusion, we observed no difference in metastatic-free survival or overall survival between $MBD4_{def}$ and M3 UM patients in contrast with the better outcome in D3 compared with M3 UMs (Figure 2, B and C). Only 1 *MBD4* carrier (UM49) had another cancer, a thyroid papillary carcinoma unrelated to *MBD4* (low TMB without CpG>TpG signature; data not shown).

Discussion

This study demonstrates that *MBD4* is a predisposing gene for UM, conferring an RR of 9.15 for this dismal disease. We further demonstrated that *MBD4* deficiency specifically predisposes to high-risk M3 UM. One surprising observation for this new cancer-predisposing condition is the absence of early-onset UM. Interestingly, the same is observed in germline *BAP1*-mutant carriers, even with the high penetrance in that context (6,23). A potential explanation for this paradox is that neither *MBD4* nor *BAP1* predisposing genes can act before a first step in the malignant transformation. This first step, presumably the Gαq-initiating event consisting of mutually exclusive activating mutations in *GNAQ*, *GNA11*, *PLCB4*, or *CYSLTR2* (26–29), would be the main determinant of age of onset (Figure 3). The second step in the malignant transformation, composed of mutations in *BAP1*, *SF3B1*, or *EIF1AX* ("BSE" events), leads to a punctuated evolution of UM (16), which would marginally influence age of onset (Figure 3). Whether *MBD4* deficiency favors malignant transformation by increasing driver mutations by modifying the methylation landscape or a distinct mechanism has yet to be determined.

Importantly, germline *MBD4* mutations were recently reported in other types of malignancy, including a polyposis-associated colorectal adenocarcinoma (20), a spiradenocarcinoma

Downloaded from https://academic.oup.com/jnci/advance-article/doi/10.1093/jnci/djaa047/5814932 by guest on 01 December 2020

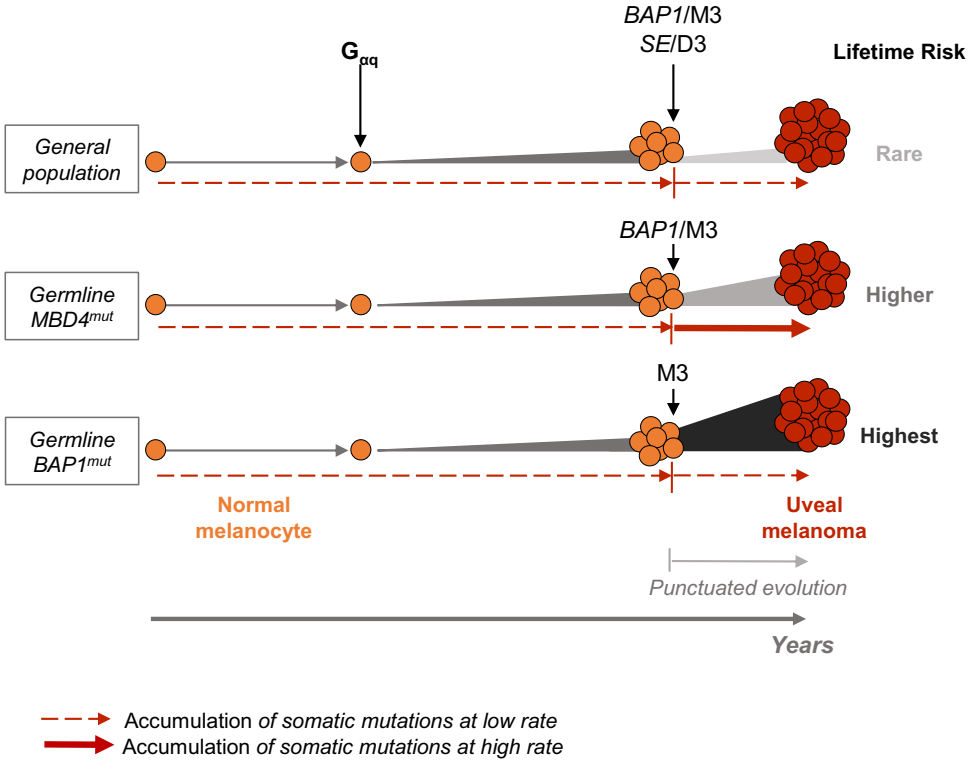


Figure 3. Working model for uveal melanoma (UM) malignant transformation process throughout time in different genetic backgrounds. Germline $MBD4^{mut}$/$BAP1^{mut}$: population with *MBD4*/*BAP1* germline mutation. Following the $G_{\alpha q}$ activating mutation, secondary mutational events in each genetic background are indicated, along with their association with either disomy 3 (D3) or monosomy 3 (M3). SE = *SF3B1* or *EIF1AX* mutation. Relative lifetime risk of UM is represented by the **expansion size and color** from normal melanocytes to UM. **Dashed and full red arrows** indicate the rate of accumulation of somatic mutations throughout time (low and high, respectively).

(19), a glioblastoma (8), a pilocytic astrocytoma, a gastric adenocarcinoma, a pancreatic adenocarcinoma, and a pancreatic endocrine tumor (21) (Table 1). Furthermore, although the above case patients were all heterozygous in the germline, biallelic germline deleterious *MBD4* mutations were reported in 3 individuals who developed acute myeloid leukemias, 2 of which had additional colonic polyposis (13). It is therefore likely that the tumor spectrum associated with *MBD4* germline mutations will expand when this gene becomes more systematically explored in clinical diagnosis. It is already clear that this spectrum mostly includes relatively rare tumors and some biological tumor features may underlie their association with *MBD4*. To be noticed, both leukemias and UMs associated with *MBD4* inactivation share a consistent inactivation of the BAP1-ASXL complex (8,13).

It should be noticed that we found no other *MBD4*-related tumors in our UM series. However, the follow-up and cohort size of this prospective series are limited, and future studies will better characterize the medical history of *MBD4* carriers. Larger cohorts will also more precisely define *MBD4* mutation frequency in UM patients and the RR conferred by these mutations. Another limitation to the study is the bias for a European population in our cohort, which reflects the higher incidence of the disease in this population (30).

Interestingly, 5 recurrent *MBD4* germline deleterious mutations were identified when taking together the LoF variants from our UM cohort and those found in public databases and reports of other cancer types: c.1706G>A [p.Trp569*] (2 patients), c.1562G>T [p.Asp521Profs*4] (4 patients), c.1443delT [p.Leu482Trpfs*9] (3 patients), c.335+1G>A [p.Arg83Profs*5] (2 patients), and c.939insA [p.Glu314Argfs*13] (2 patients) (Table 1), suggesting founder mutations. Furthermore, the observation of different tumor types associated with the same *MBD4* germline mutation suggests a more global role of *MBD4* in cancer predisposition. The peculiar UM proneness in *MBD4*-mutant carriers (13 out of 23 carriers; Table 1) remains unexplained, but the fact that the frequent M3 in UM inactivates wild-type copies of both *BAP1* and *MBD4* suppressor genes may at least in part explain the frequent inactivation of *MBD4* in UM.

In summary, we described here a novel autosomal-dominant syndrome that is caused by germline mutations of *MBD4*, characterized by a high RR of developing hypermutated UM and possibly other malignancies. Tumors arising in such a context are associated with a CpG>TpG mutator phenotype and have clinical relevance because they may respond to immune-checkpoint inhibitors.

Funding

Supported by funding from the European Commission under the Horizon 2020 program and innovation program under the Marie Skłodowska-Curie grant agreement No 666003 (A-CD), the Horizon 2020 program UM Cure (LM; Project number: 667787), the INCa/ITMO/AVIESAN PhD fellowship program "*Formation à la recherche translationelle*" (MR), the *Ligue Nationale Contre le Cancer* (AE), the *Institut National de la Santé et de la Recherche Médicale* (INSERM), the Institut Curie, the *Ligue Nationale Contre le Cancer* (*Labellisation*), the *Programme de Recherche Translationnelle en Cancérologie* (PRT-K19-51) INCa-DGOS, and the *Site de Recherche Intégrée sur le*

Downloaded from https://academic.oup.com/jnci/advance-article/doi/10.1093/jnci/djaa047/5810647 by guest on 01 December 2020

Cancer (SiRIC) de l'Institut Curie. The Institut Curie ICGex NGS platform is funded by the EQUIPEX "*investissements d'avenir*" program (ANR-10-EQPX- 03) and ANR10-INBS-09–08 from the *Agence Nationale de le Recherche*.

Notes

Role of the funder: The funders had no role in the design of the study; the collection, analysis, and interpretation of the data; the writing of the manuscript; and the decision to submit the manuscript for publication.

Disclosures: The authors have no conflict of interest to declare except for the following: M.R. received a grant support from Bristol-Myers Squibb and Merck.

Author contributions: A.-C.D. and M.R. conceived the study, performed experiments, interpreted the data and wrote the manuscript. A.E. and A.H. performed bioinformatics analyses. L.M., S.A., A.E.-M. and G.P. interpreted the data and provided critical advice. O.M., A.M., S.G. and N.C. provided patients specimens and critical advice. S.D., D.L. and G.P. performed biological analyses. C.C. provided clinical data and critical advice. M.-H.S. conceived and guided the study, interpreted the data and wrote the manuscript. All authors reviewed and approved the final manuscript.

Acknowledgment: The authors thank Joshua J. Waterfall for his insightful comments.

References

1. Aronow ME, Topham AK, Singh AD. Uveal melanoma: 5-year update on incidence, treatment, and survival (SEER 1973-2013). *Ocul Oncol Pathol*. 2018;4(3):145–151.
2. Khoja L, Atenafu EG, Suciu S, et al. Meta-analysis in metastatic uveal melanoma to determine progression free and overall survival benchmarks: an international rare cancers initiative (IRCI) ocular melanoma study. *Ann Oncol*. 2019;30(8):1370–1380.
3. Carvajal RD, Schwartz GK, Tezel T, et al. Metastatic disease from uveal melanoma: treatment options and future prospects. *Br J Ophthalmol*. 2017;101(1):38–44.
4. Harbour JW, Onken MD, Roberson EDO, et al. Frequent mutation of BAP1 in metastasizing uveal melanomas. *Science*. 2010;330(6009):1410–1413.
5. Wiesner T, Murali R, Fried I, et al. A distinct subset of atypical Spitz tumors is characterized by BRAF mutation and loss of BAP1 expression. *Am J Surg Pathol*. 2012;36(6):818–830.
6. Walpole S, Pritchard AL, Cebulla CM, et al. Comprehensive study of the clinical phenotype of germline BAP1 variant-carrying families worldwide. *J Natl Cancer Inst*. 2018;110(12):1328–1341.
7. Furney SJ, Pedersen M, Gentien D, et al. SF3B1 mutations are associated with alternative splicing in uveal melanoma. *Cancer Discov*. 2013;3(10):1122–1129.
8. Rodrigues M, Mobuchon L, Houy A, et al. Outlier response to anti-PD1 in uveal melanoma reveals germline MBD4 mutations in hypermutated tumors. *Nat Commun*. 2018;9(1):1866.
9. Johansson PA, Stark A, Palmer JM, et al. Prolonged stable disease in a uveal melanoma patient with germline MBD4 nonsense mutation treated with pembrolizumab and ipilimumab. *Immunogenetics*. 2019;71(5–6):433–436.
10. Hendrich B, Hardeland U, Ng HH, et al. The thymine glycosylase MBD4 can bind to the product of deamination at methylated CpG sites. *Nature*. 1999;401(6750):301–304.
11. Yoon JH, Iwai S, O'Connor TR, et al. Human thymine DNA glycosylase (TDG) and methyl-CpG-binding protein 4 (MBD4) excise thymine glycol (Tg) from a Tg: G mispair. *Nucleic Acids Res*. 2003;31(18):5399–5404.
12. Alexandrov LB, Kim J, Haradhvala NJ, et al. PCAWG Mutational Signatures Working Group. The repertoire of mutational signatures in human cancer. *Nature*. 2020;578(7793):94–101.
13. Sanders MA, Chew E, Flensburg C, et al. MBD4 guards against methylation damage and germ line deficiency predisposes to clonal hematopoiesis and early-onset AML. *Blood*. 2018;132(14):1526–1534.
14. Hashimoto H, Liu Y, Upadhyay AK, et al. Recognition and potential mechanisms for replication and erasure of cytosine hydroxymethylation. *Nucleic Acids Res*. 2012;40(11):4841–4849.
15. Rothman KJ. *Epidemiology, an Introduction*. 2nd ed. New York, NY: Oxford University Press; 2002.
16. Field MG, Durante MA, Anbunathan H, et al. Punctuated evolution of canonical genomic aberrations in uveal melanoma. *Nat Commun*. 2018;9(1):116.
17. Robertson AG, Shih J, Yau C, et al. Integrative analysis identifies four molecular and clinical subsets in uveal melanoma. *Cancer Cell*. 2017;32(2):204–220.e15.
18. Rodrigues M, Mobuchon L, Houy A, et al. Evolutionary routes in metastatic uveal melanomas depend on MBD4 alterations. *Clin Cancer Res*. 2019;25(18):5513–5524.
19. Davies HR, Hodgson K, Schwalbe E, et al. Epigenetic dysregulation underpins tumorigenesis in a cutaneous tumor syndrome. bioRxiv 2019; doi: 10.1101/687459.
20. Tanakaya K, Kumamoto K, Tada Y, et al. A germline MBD4 mutation was identified in a patient with colorectal oligopolyposis and early-onset cancer: a case report. *Oncol Rep*. 2019;42(3):1133–1140.
21. Waszak SM, Tiao G, Zhu B, et al. Germline determinants of the somatic mutation landscape in 2,642 cancer genomes. bioRxiv 2017; doi: 10.1101/208330.
22. Morera S, Grin I, Vigouroux A, et al. Biochemical and structural characterization of the glycosylase domain of MBD4 bound to thymine and 5-hydroxymethyuracil-containing DNA. *Nucleic Acids Res*. 2012;40(19):9917–9926.
23. Gupta MP, Lane AM, DeAngelis MM, et al. Clinical characteristics of uveal melanoma in patients with germline BAP1 mutations. *JAMA Ophthalmol*. 2015;133(8):881–887.
24. Prescher G, Bornfeld N, Hirche H, et al. Prognostic implications of monosomy 3 in uveal melanoma. *Lancet*. 1996;347(9010):1222–1225.
25. Singh AD, De Potter P, Fijal BA, et al. Lifetime prevalence of uveal melanoma in white patients with oculo(dermal) melanocytosis. *Ophthalmology*. 1998;105(1):195–198.
26. Johansson P, Aoude LG, Wadt K, et al. Deep sequencing of uveal melanoma identifies a recurrent mutation in PLCB4. *Oncotarget*. 2016;7(4):4624–4631.
27. Van Raamsdonk CD, Bezrookove V, Green G, et al. Frequent somatic mutations of GNAQ in uveal melanoma and blue naevi. *Nature*. 2009;457(7229):599–602.
28. Van Raamsdonk CD, Griewank KG, Crosby MB, et al. Mutations in GNA11 in uveal melanoma. *N Engl J Med*. 2010;363(23):2191–2199.
29. Moore AR, Ceraudo E, Sher JJ, et al. Recurrent activating mutations of G-protein-coupled receptor CYSLTR2 in uveal melanoma. *Nat Genet*. 2016;48(6):675–680.
30. Mobuchon L, Battistella A, Bardel C, et al. A GWAS in uveal melanoma identifies risk polymorphisms in the CLPTM1L locus. *NPJ Genom Med*. 2017;2(1):1–7.

ARTICLE

Downloaded from https://academic.oup.com/jnci/advance-article/doi/10.1093/jnci/djaa047/5814932 by guest on 01 December 2020